

# Dehydrogenation of a Combined LiAlH<sub>4</sub>/LiNH<sub>2</sub> System

Jun Lu and Zhigang Zak Fang\*

Department of Metallurgical Engineering, University of Utah, 135 South 1460 East Room 412, Salt Lake City, Utah 84112

Received: July 18, 2005; In Final Form: August 27, 2005

Although there have been numerous materials systems studied as potential candidates for hydrogen storage applications, none of the materials known to date has demonstrated enough hydrogen capacity or efficiency at required operating temperature ranges. There are still considerable opportunities for discovery of new materials or material systems that could lead to advances in science as well as commercial technologies in this area. LiAlH<sub>4</sub> is one of the most promising materials owing to its high hydrogen content. In the present work, we investigated dehydrogenation properties of the combined system of LiAlH<sub>4</sub> and LiNH<sub>2</sub> under atmospheric argon. Thermogravimetric analysis (TGA) of 2LiAlH<sub>4</sub>/LiNH<sub>2</sub> mixtures without any catalysts indicated that a large amount of hydrogen (~8.1 wt %) can be released between 85 and 320 °C under a heating rate of 2 °C/min in three dehydrogenation reaction steps. It is found that LiNH<sub>2</sub> effectively destabilizes LiAlH<sub>4</sub> by reacting with LiH during the dehydrogenation process of LiAlH<sub>4</sub>.

## 1. Introduction

As a promising clean fuel for vehicles, hydrogen can be used for propulsion, either directly or in fuel cells. In both cases, a suitable hydrogen-storage material is needed to make this source of energy economically viable. Although there have been numerous materials systems studied as potential candidates for hydrogen storage applications, none of the materials known to date have demonstrated sufficient hydrogen capacity or efficiency at required operating temperature ranges. There are still considerable opportunities for discovery of new materials or material systems that could lead to advances in science as well as commercial technologies in this area.

Following the break-through work on Ti-doped NaAlH<sub>4</sub> by Bogdanovic and Schwickardi in 1997,<sup>1</sup> alkali- and alkaline-earth-metal-based complex aluminum hydrides, such as MAIH<sub>4</sub> (M = Li,<sup>2–6</sup> Na,<sup>7–14</sup> K<sup>15</sup>), have been studied intensively as possible candidate materials for high-capacity reversible hydrogen storage. It has been generally found that alkali-based aluminum hydrides have great potential for storing hydrogen at moderate temperatures and pressures. Among them, LiAlH<sub>4</sub>, which was first synthesized in 1947<sup>16</sup> and is used as a powerful reducing agent in organic chemistry,<sup>17</sup> is one of the materials having the highest inherent hydrogen capacity. Its total hydrogen content is approximately 10.6 wt %.

In addition to the inherent hydrogen storage capacity, critical requirements for any solid hydrogen storage materials include the reversibility of hydrogen release and uptake reactions and the kinetics of these reactions. During decomposition at elevated temperatures, lithium alanate, LiAlH<sub>4</sub>, first reduces to intermediate compounds Li<sub>3</sub>AlH<sub>6</sub> and then to LiH at around 160 to 210 °C, and liberates 5.3 and 2.6 wt % of hydrogen, respectively.<sup>18–22</sup> The dehydrogenation of LiH, however, occurs at much higher temperatures, around 720 °C,<sup>23</sup> liberating another 2.6 wt % of hydrogen. This temperature is too high, and hence the decomposition of LiH is not considered viable for practical purposes.

Thus, the maximum potential hydrogen storage capacity of LiAlH<sub>4</sub> decreases to 7.9 wt % for LiAlH<sub>4</sub>. Clearly, the difficulty of releasing H<sub>2</sub> from LiH limits the practical hydrogen capacity of lithium alanates. It is noted that the same problem also exists for the NaAlH<sub>4</sub> system.

Recently, Chen et al.<sup>24</sup> and Hu and Ruckenstein<sup>25</sup> investigated the potential of lithium nitride, Li<sub>3</sub>N, as a promising hydrogen storage material, in which the hydrogenation and dehydrogenation are accomplished by the following two-step reversible reactions (R1 and R2):<sup>26</sup>



LiNH<sub>2</sub> and LiH are used as the starting materials, and the dehydrogenation temperature is around 200 to 430 °C in a vacuum, based on the literature.<sup>24–26</sup>

As mentioned earlier, the utility of LiAlH<sub>4</sub> is limited because the temperature for dehydrogenation of LiH is too high. However, reactions 1 and 2 suggest that the dehydrogenation temperature of LiH can be decreased dramatically when it is combined with LiNH<sub>2</sub>.<sup>24–26</sup> It is therefore hypothesized that, if LiAlH<sub>4</sub> and LiNH<sub>2</sub> are combined, the LiH that forms as an intermediate product of the dehydrogenation of LiAlH<sub>4</sub> can then react with LiNH<sub>2</sub> to release H<sub>2</sub> at a low temperature. In other words, all the hydrogen contained in LiAlH<sub>4</sub> can be released, which could raise the effective hydrogen storage capacity of LiAlH<sub>4</sub>. In the present work, the dehydrogenation reactions of LiAlH<sub>4</sub> were studied by combining it with LiNH<sub>2</sub>. The new combined system (2LiAlH<sub>4</sub>/LiNH<sub>2</sub>) has a very high inherent hydrogen capacity—10.1 wt %, theoretically. The characteristics of dehydrogenation reactions of the combined system are compared with that of LiAlH<sub>4</sub> and LiNH<sub>2</sub>/2LiH. The effects of doping on the combined reactions are also investigated.

## 2. Experimental Section

The starting materials, lithium aluminum hydride (LiAlH<sub>4</sub>, 95%), lithium amide (LiNH<sub>2</sub>, 95%), and TiCl<sub>3</sub>–1/3AlCl<sub>3</sub>, were

\* Address correspondence to this author. E-mail: zfang@mines.utah.edu. Phone: (801) 581-8128. Fax: (801) 581-4937.

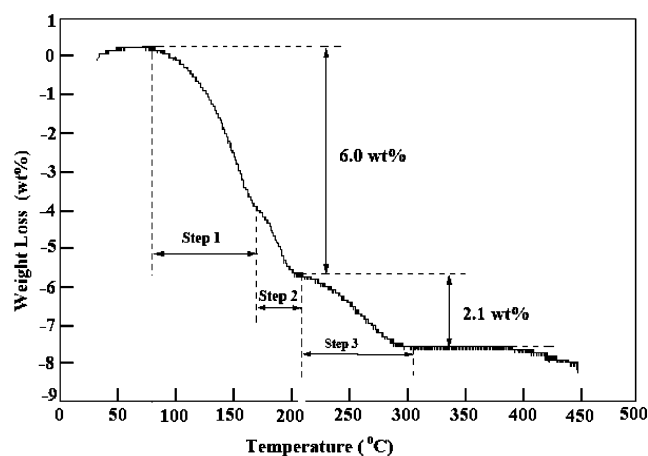


**Figure 1.** TGA curves of 2LiAlH<sub>4</sub> + LiNH<sub>2</sub> (sample 1) under atmospheric argon and a heating rate of 2 °C/min.

purchased from Aldrich Chemical and used as received without any further purification. To prevent samples and raw materials from undergoing oxidation and/or hydroxide formation, they were stored and handled in a nitrogen-filled glovebox.

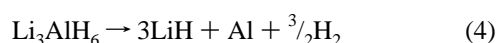
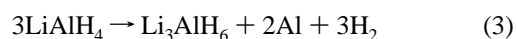
A mixture of LiAlH<sub>4</sub> and LiNH<sub>2</sub> with a molar ratio of 2:1 was ground by hand in a mortar for 10 min (designated as sample 1). Another mixture of 2LiAlH<sub>4</sub>/LiNH<sub>2</sub>/TiCl<sub>3</sub>–<sup>1</sup>/<sub>3</sub>AlCl<sub>3</sub> was obtained by further grinding the above mixture with 4 wt % of TiCl<sub>3</sub>–<sup>1</sup>/<sub>3</sub>AlCl<sub>3</sub> for 5 min (designated as sample 2).

The thermal gas desorption properties of the mixtures were determined by thermogravimetry analyzer (TGA) (Shimadzu TGA50) upon heating to 450 °C at a heating rate of 2 °C/min. To avoid any exposure of the sample to air, this equipment was set inside the nitrogen-filled glovebox equipped with a recirculation system.

The identification of reactants and reaction products in the mixture before and after thermogravimetric analysis was carried out with a Siemens D5000 model X-ray diffractometer with Ni-filtered Cu Kα radiation ( $\lambda = 1.5406 \text{ \AA}$ ). A scanning rate of 0.02 deg/s was applied to record the patterns in the  $2\theta$  range of 10° to 90°. In addition, it is noted that the amorphous-like background in the XRD patterns is attributed to the thin plastic films that were used to cover the powders.

### 3. Results and Discussion

**3.1. Desorption Properties of 2LiAlH<sub>4</sub>/LiNH<sub>2</sub>.** Figure 1 shows the TGA result of the 2LiAlH<sub>4</sub>/LiNH<sub>2</sub> without catalyst (sample 1). The sample was run under argon atmosphere with a heating rate of 2 °C/min. Temperatures are held constant at time points when there is a definitive weight loss indicating a decomposition reaction until the reaction step is complete. Each reaction step is identified by the changes of the rate of the weight loss. It can be seen that a total of 8.1 wt % of hydrogen was released within the examined temperature range. The desorption process appears to consist of three steps: The first two steps are in the temperature range of 85 to 200 °C. A total of 6.0 wt % of hydrogen was released within these two steps. These two weight-loss steps can best be described by the following reactions (R3 and R4):



The third step occurs at above 210 °C. Another 2.1 wt % of hydrogen was desorbed during the third step, which corresponds

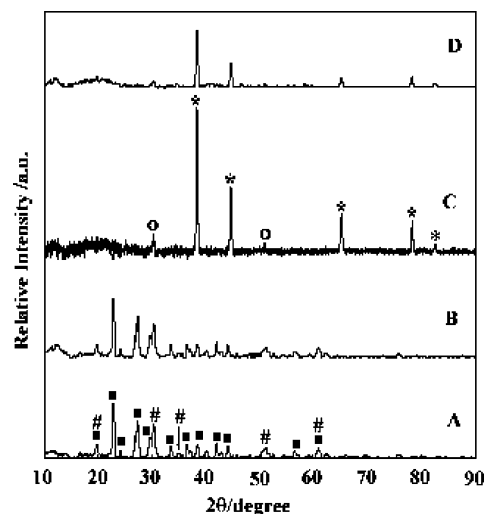
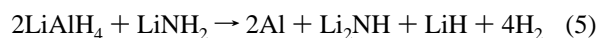


**Figure 2.** XRD patterns of (A) sample 1 before dehydrogenation, (B) sample 2 before dehydrogenation, (C) sample 1 after dehydrogenation, and (D) sample 2 after dehydrogenation.

to reaction 1. Thus, the overall reaction for the combined LiAlH<sub>4</sub> and LiNH<sub>2</sub> system can be given as (R5):



To verify these specific reaction steps, X-ray diffraction analysis was carried out on the raw materials as well as on the reaction products. Figure 2 shows the XRD patterns of selected samples before and after dehydrogenation. Crystalline phases are identified by comparing the experimental data with JCPDS files from the International Center for Diffraction Data. In Figure 2A, which shows the XRD pattern of sample 1 before dehydrogenation, the peaks marked with closed squares are attributed to the phase of monoclinic LiAlH<sub>4</sub>, and those marked with hashes are attributed to the phase of tetragonal LiNH<sub>2</sub>. Figure 2B shows the XRD pattern of sample 2 before dehydrogenation. No characteristic peaks of crystalline TiCl<sub>3</sub> or AlCl<sub>3</sub> are observed, which is possibly due to their low contents. Figures 2C and 2D show the XRD patterns of samples 1 and 2, respectively, after dehydrogenation. The XRD patterns clearly show that LiAlH<sub>4</sub> and LiNH<sub>2</sub> are absent in the samples, indicating that they are consumed by the decomposition and some new compounds formed. In these figures, the peaks that are marked with open circles are indexed to be the cubic phase of Li<sub>2</sub>NH, and those marked with asterisks are indexed to be Al or Al + LiH (Al and LiH peaks overlap on the XRD patterns). However, because only Li<sub>2</sub>NH, and not Li<sub>3</sub>N, exists after dehydrogenation, these peaks are indexed to be the mixture of Al + LiH, based on the reaction between LiH and LiNH<sub>2</sub>.<sup>24,26</sup>

Figure 2 confirms the overall dehydrogenation (R5) by identification of the final reaction products. However, it does not provide any information regarding the reaction path. To determine the reaction paths, i.e., the intermediate reactions, two approaches were taken. First, R3 and R4 are proposed as the intermediate reactions because the molar balance of these reactions matches with the weight loss reaction steps as indicated by the TGA curve in Figure 1. To further confirm each reaction step, the intermediate products after partial dehydrogenation at specific temperatures were analyzed with XRD. Figure 3A shows the XRD pattern of the product after dehydrogenation at 100 °C for 20 min, in which the peaks that are marked with open circles are indexed to be monoclinic Li<sub>3</sub>AlH<sub>6</sub>, those marked

TABLE 1: The Dehydrogenation Temperature and Hydrogen Capacity for Different Systems

	LiAlH <sub>4</sub>	LiAlH <sub>4</sub> + 4 wt % TiCl <sub>3</sub> -AlCl <sub>3</sub>	2LiH + LiNH <sub>2</sub>	2LiAlH <sub>4</sub> + LiNH <sub>2</sub>	2LiAlH <sub>4</sub> + LiNH <sub>2</sub> + 4 wt % TiCl <sub>3</sub> -AlCl <sub>3</sub>
step 1 (°C/wt %)	170/4.4	140/4.4	220/6.0	85/4.0	95/3.8
step 2 (°C/wt %)	200/2.0	165/2.2		165/2.0	140/2.1
step 3 (°C/wt %)				200/2.1	205/2.2
total wt % H <sub>2</sub>	6.4	6.6	6.0	8.1	8.1

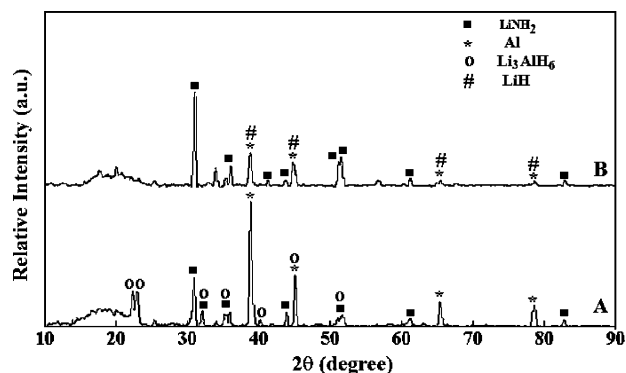


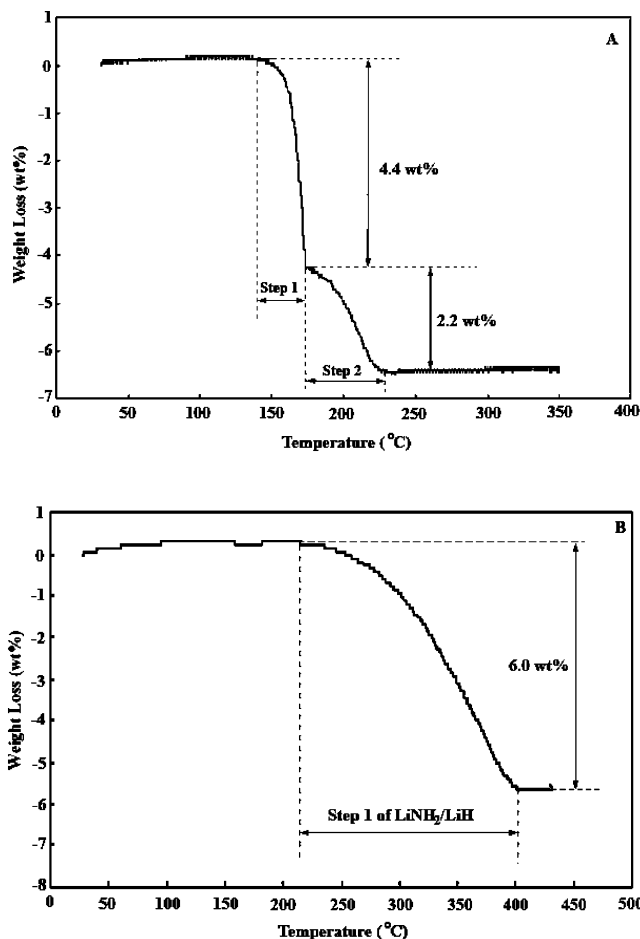
Figure 3. XRD patterns of (A) sample 1 after heating to 100 °C and (B) sample 1 after heating to 150 °C.

with asterisks are indexed to be cubic aluminum, and those marked with closed squares are indexed to be tetragonal LiNH<sub>2</sub>. This confirms that the first dehydrogenation step corresponds to R3.

Figure 3B is the XRD pattern of the product after dehydrogenation at 150 °C for 20 min. It clearly shows that the sample contains LiNH<sub>2</sub> (marked with closed squares); however, Li<sub>3</sub>AlH<sub>6</sub> is absent. The peaks that are marked with asterisks and hashes are indexed to be Al + LiH. This result confirms reaction 4. Therefore, the overall reaction path follows R3, R4, and R1.

**3.2. Comparison of the Current System to LiAlH<sub>4</sub> and 2LiH + LiNH<sub>2</sub>.** To compare the kinetics of the dehydrogenation of the combined system (2LiAlH<sub>4</sub>/LiNH<sub>2</sub>) with that of the LiAlH<sub>4</sub> and LiNH<sub>2</sub>/2LiH systems, TGA experiments were carried out with LiAlH<sub>4</sub>, Ti-doped LiAlH<sub>4</sub>, and LiNH<sub>2</sub>/LiH under the same conditions as described for 2LiAlH<sub>4</sub>/LiNH<sub>2</sub>. Figure 4 shows the TGA results of Ti-doped LiAlH<sub>4</sub> and LiNH<sub>2</sub>/2LiH. Primary characteristics of dehydrogenation processes include the temperature and the percentage of hydrogen released for each step of the process. Table 1 compares these characteristics among the Ti-doped LiAlH<sub>4</sub>, LiNH<sub>2</sub>/2LiH, and 2LiAlH<sub>4</sub>/LiNH<sub>2</sub> systems. Table 1 shows that the dehydrogenation temperature of the 2LiAlH<sub>4</sub>/LiNH<sub>2</sub> system is lower than that of either the Ti-doped LiAlH<sub>4</sub> or LiNH<sub>2</sub>/2LiH systems. The percent of hydrogen released from the combined system is also higher than that from Ti-doped LiAlH<sub>4</sub> or LiNH<sub>2</sub>/2LiH.

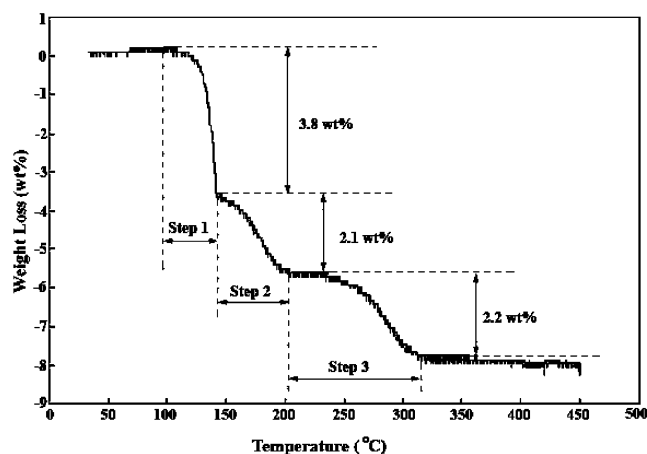
It is important to note that the current results for the LiNH<sub>2</sub>/2LiH system differ from those reported by Chen et al.<sup>24–26</sup> The differences are attributed to the fact that the dehydrogenation experiments reported by Chen et al. were carried out in a vacuum, while the current study was carried out in atmospheric argon. Theoretically, the hydrogen storage capacity of the combined system is 10.1 wt % if the dehydrogenation is complete with a fourth reaction step as described in reaction 2. During Chen's experiment, reaction 2 was observed within the temperature range of 320 to 430 °C under vacuum. However, current results for the LiNH<sub>2</sub>/2LiH system show that the percent of hydrogen decreases to 6.0% when the experiment is conducted under atmospheric pressure within the temperature range of room temperature to 450 °C. This suggests that the

Figure 4. TGA curves of (A) TiCl<sub>3</sub>-1/3AlCl<sub>3</sub> doped LiAlH<sub>4</sub> and (B) 2LiH + LiNH<sub>2</sub> under atmospheric argon and a heating rate of 2 °C/min.

fourth step, R2, does not occur in the combined system under the experimental conditions of this study, which explains why the total percent of hydrogen released is 8.1 wt %.

Although the percent of hydrogen released from the combined system is lower than its maximum potential within the temperature range used during this study, current results demonstrate that the kinetics of dehydrogenation of LiAlH<sub>4</sub> can be improved by combining it with LiNH<sub>2</sub>. The effects of LiNH<sub>2</sub> are 2-fold. First, the temperature for dehydrogenation reaction 3 is lower than that of LiAlH<sub>4</sub> when it is heated alone. This suggests an interaction between light metal amide and alanate group (e.g. AlH<sub>4</sub><sup>-</sup>) that changes the thermodynamics of the reactions by either lowering the enthalpy of the dehydrogenation reaction or tipping the balance of the reaction toward one direction. This is a fundamentally different reaction mechanism from the decomposition of alanates when they are heated alone. Second, the hydrogen combined in LiH can be liberated by reaction with LiNH<sub>2</sub>, which increases the effective hydrogen capacity of LiAlH<sub>4</sub>.

The thermodynamic effects of lithium amide on the overall reaction can be further understood by examining the reaction



**Figure 5.** TGA curves of TiCl<sub>3</sub>–<sup>1</sup>/<sub>3</sub>AlCl<sub>3</sub> doped 2LiAlH<sub>4</sub> + LiNH<sub>2</sub> (sample 2) under atmospheric argon and a heating rate of 2 °C/min.

constant of R4. In general, the free energy of reaction can be described by the following expression

$$\Delta_r G_m = -RT \ln K^\phi + RT \ln Q \quad (6)$$

where  $Q$  is the activity quotient and  $K^\phi$  is the equilibrium constant. Specifically for R4,

$$K^\phi = \frac{(\alpha_{\text{LiH}})^2 \cdot (\alpha_{\text{Al}})^{2/3} \cdot (\rho_{\text{H}_2})_e}{(\alpha_{\text{Li}_3\text{AlH}_6})^{2/3}_e} \quad (7)$$

$$Q = \frac{(\alpha_{\text{LiH}})^2 \cdot (\alpha_{\text{Al}})^{2/3} \cdot (\rho_{\text{H}_2})}{(\alpha_{\text{Li}_3\text{AlH}_6})^{2/3}} \quad (8)$$

when  $Q < K^\phi$  and  $\Delta_r G_m < 0$  the reaction moves toward the right spontaneously,  $Q = K^\phi$  and  $\Delta_r G_m = 0$  the reaction is at equilibrium, and  $Q > K^\phi$  and  $\Delta_r G_m > 0$  the reversible reaction occurs spontaneously.

When lithium amide is added to the system,  $Q$  decreases as R1 and R2 proceed, which is in turn beneficial for dehydrogenation via R4. It should be noted that to further understand the destabilization effect of LiNH<sub>2</sub> on LiAlH<sub>4</sub>, thermodynamic data including reaction enthalpies, entropies, and free energies of each reaction step are needed. These data can be determined either through experiments or modeling such as first-principle (FP) calculations, which is beyond the scope of the present study. As an example, the dehydrogenation of NaAlH<sub>4</sub>, Na<sub>3</sub>AlH<sub>6</sub>, and NaH was investigated recently by Ke and Tanaka<sup>27</sup> using FP technique.

**3.3. Effect of TiCl<sub>3</sub>–<sup>1</sup>/<sub>3</sub>AlCl<sub>3</sub> Doping.** It is well-known now that the potential of sodium alanate (NaAlH<sub>4</sub>) for hydrogen storage applications is dependent upon doping NaAlH<sub>4</sub> with a Ti species. Ti doping improves the kinetics of the reversible hydrogen release and uptake reactions of NaAlH<sub>4</sub>. To study any possible effects of doping on the dehydrogenation of the combined 2LiAlH<sub>4</sub>/LiNH<sub>2</sub> system, a mixture of LiAlH<sub>4</sub> and LiNH<sub>2</sub> doped with TiCl<sub>3</sub>–<sup>1</sup>/<sub>3</sub>AlCl<sub>3</sub> (Sample 2) was analyzed by using TGA, as shown in Figure 5. It can be seen that, within the experimented temperature range, hydrogen desorbs from this mixture with rather similar behavior to that of sample 1, which is the same material without doping. Characteristic temperatures and percent of hydrogen release of doped 2LiAlH<sub>4</sub>/LiNH<sub>2</sub> are also listed in Table 1. It shows that the doping does not affect the kinetics of the combined 2LiAlH<sub>4</sub>/LiNH<sub>2</sub> system signifi-

cantly, while TiCl<sub>3</sub>–<sup>1</sup>/<sub>3</sub>AlCl<sub>3</sub> doping is very effective in reducing the dehydrogenation temperature of LiAlH<sub>4</sub> when used alone. The latter is in agreement with the literature.<sup>3,4</sup> In the current experiment, the dehydrogenation of LiAlH<sub>4</sub> from sample 1 takes place at almost same temperature as that of sample 2, which suggests that LiNH<sub>2</sub> acts as a destabilizer for decomposition of LiAlH<sub>4</sub>. This is an important implication that could be useful for destabilizing other alkali aluminum hydride systems.

Finally, it is important to note that the reversibility of a solid hydride material is one of the most important properties of the material, determining its potential for practical applications. Although the current study did not address the reversibility issues directly, there are indications from the literature that the hydrogen release-and-uptake reactions of the combined 2LiAlH<sub>4</sub>/LiNH<sub>2</sub> system should be reversible.<sup>3,24–26</sup> However, it is obviously essential that the reversibility of the current system be demonstrated directly, which is a focus of the ongoing efforts of the present authors. In addition, although the current system shows great potential for hydrogen storage applications, the temperatures of dehydrogenation reactions of this system are still too high, particularly for the second and third steps. Further studies are needed to improve the kinetics of dehydrogenation reactions.

#### 4. Summary

The dehydrogenation of a combined system of LiAlH<sub>4</sub> and LiNH<sub>2</sub> under atmospheric argon was studied.<sup>28</sup> Thermogravimetric analysis (TGA) of LiAlH<sub>4</sub>/LiNH<sub>2</sub> mixtures without any catalysts indicated that a large amount of hydrogen (~8.1 wt %) can be released between 85 and 320 °C under a heating rate of 2 °C/min in three dehydrogenation reaction steps. The results also showed that the dehydrogenation temperature of the LiAlH<sub>4</sub>/LiNH<sub>2</sub> system is lower than that of either Ti-doped LiAlH<sub>4</sub> or LiNH<sub>2</sub>/2LiH. The percent of hydrogen released from the 2LiAlH<sub>4</sub>/LiNH<sub>2</sub> mixture is also higher than that from LiAlH<sub>4</sub> or LiNH<sub>2</sub>/LiH. The results also show that LiNH<sub>2</sub> destabilizes LiAlH<sub>4</sub>.

**Acknowledgment.** This research is partially made possible by the start-up fund provided by the College of Mines and Earth Sciences of the University of Utah. We also received financial support from the U.S. Department of Energy (DOE) under contract no. DE-FC36-05GO15069 since March 2005.

#### References and Notes

- Bogdanovic, B.; Schwickardi, M. *J. Alloys Compd.* **1997**, 253, 1.
- Balema, V. P.; Dennis, K. W.; Pecharsky, V. K. *Chem. Commun.* **2000**, 17, 1665.
- Chen, J.; Kuriyama, N.; Xu, Q.; Takeshita, H. T.; Sakai, T. *J. Phys. Chem. B* **2001**, 105, 11214.
- Blanchard, D.; Brinks, H. W.; Hauback, B. C.; Norby, P. *Mater. Sci. Eng. B* **2004**, 108, 54.
- Brinks, H. W.; Hauback, B. C.; Norby, P.; Fjellvåg, H. *J. Alloys Compd.* **2003**, 351, 222.
- Hauback, B. C.; Brinks, H. W.; Fjellvåg, H. *J. Alloys Compd.* **2002**, 346, 184.
- Zidan, R. A.; Taraka, S.; Hee, A. G.; Jensen, C. M. *J. Alloys Compd.* **1999**, 285, 119.
- Zaluska, A.; Zaluski, L.; Strom-Olsen, J. O. *J. Alloys Compd.* **2000**, 298, 125.
- Bogdanovic, B.; Schwickardi, M. *Appl. Phys. A* **2001**, 72, 221.
- Jensen, C. M.; Gross, K. J. *Appl. Phys. A* **2001**, 72, 213.
- Sandrock, G.; Gross, K. J.; Thomas, G. *J. Alloys Compd.* **2002**, 339, 299.
- Sun, D. L.; Kiyobayashi, T.; Takeshita, H. T.; Kuriyama, N.; Jensen, C. M. *J. Alloys Compd.* **2002**, 337, 8.
- Kiyobayashi, T.; Srinivasan, S.; Sun, D. L.; Jensen, C. M. *J. Phys. Chem. A* **2003**, 107, 7671.



- (14) Brinks, H. W.; Jensen, C. M.; Srinivasan, S. S.; Hauback, B. C.; Blanchard, D.; Murphy, K. *J. Alloys Compd.* **2004**, *376*, 215.
- (15) Morioka, H.; Kakizaki, K.; Chung, S. C.; Yamada, A. *J. Alloys Compd.* **2003**, *353*, 310.
- (16) Finholt, A. E.; Bond, A. C., Jr.; Schlesinger, H. I. *J. Am. Chem. Soc.* **1947**, *69*, 1199.
- (17) Rittmeyer, P. *Chim. Oggi (Chem. Today)* **1995**, *13*, 51.
- (18) Garner, W. E.; Haycock, E. W. *Proc. R. Soc. Ser. A* **1952**, *211*, 335.
- (19) Mikheeva, V. I.; Selivokhina, M. S.; Kryukova, O. N. *Dokl. Akad. Nauk SSSR* **1956**, *109*, 439.
- (20) Block, J.; Gray, A. P. *Inorg. Chem.* **1965**, *4*, 104.
- (21) Dils, J. A.; Ashby, E. C. *Inorg. Chem.* **1972**, *11*, 1230.
- (22) Bastide, J. P.; Bonnetot, B.; Letoffe, J. M.; Claudy, P. *Mater. Sci. Bull.* **1985**, *20*, 997.
- (23) Grochala, W.; Edwards, P. *Chem. Rev.* **2004**, *104*, 1283.
- (24) Chen, P.; Xiong, Z.; Luo, J.; Lin, J.; Tan, K. L. *Nature* **2002**, *420*, 302.
- (25) Hu, Y. H.; Ruckenstein, E. *Ind. Eng. Chem. Res.* **2003**, *42*, 5135.
- (26) Chen, P.; Xiong, Z.; Luo, J.; Lin, J.; Tan, K. L. *J. Phys. Chem. B* **2003**, *107*, 10967.
- (27) Ke, X.; Tanaka, I. *Phys. Rev. B* **2005**, *71*, 024117–1.
- (28) During the revision process of this paper, it came to our attention from one of the referees that a similar concept was presented during the 9th International Conference on Advanced Materials (ICAM, ICMAT, July 3–8, 2005, Singapore) by Zhitao Xiong, Guotao Wu, JianJiang Hu, and Ping Chen. It is noted that the present work and the work by Xiong et al. are independent of each other.